Available online at www.sciencedirect.com
SCIENCE DIRECT
NDT&E International 39 (2006) 109–116
NDT&E international
www.elsevier.com/locate/ndteint

The embedment of fiber Bragg grating sensors into filament wound pressure tanks considering multiplexing

D.H. Kang[a,*], C.U. Kim[b], C.G. Kim[c]

[a]Railway Interoperability Research Team, Korea Railroad Research Institute, 360-1, Woram-dong, Uiwang-si, Gyeonggi-do 437-757, South Korea
[b]Vehicle CAE Team, R&D Division, Hyundai-Kia Motors, 772-1, Jangduk-dong, Hwaseong-si, Gyeonggi-do 445-706, South Korea
[c]Division of Aerospace Engineering, Korea Advanced Institute of Science and Technology, 373-1, Guseong-dong, Yuseong-gu, Daejeon 305-701, South Korea

Received 1 July 2005; revised 27 July 2005; accepted 27 July 2005
Available online 23 September 2005

Abstract

Filament wound pressure tanks are under high internal pressure during the operation and it has the complexity in damage mechanism and failure modes. For this reason, it is necessary to monitor the tank through its operation as well as during the whole fabrication process. A large number of sensors must be embedded into multiple positions of the tank from its fabrication step for monitoring the whole tank. Fiber optic sensors, especially fiber Bragg grating (FBG) sensors are widely used for various applications because of good multiplexing capabilities. However, we need to develop the embedding technique of FBG sensors into harsh inner environment of the tank for the successful embedment. In this paper, we studied the embedding technique of a number of FBG sensors into filament wound pressure tanks considering multiplexing and conducted in situ structural health monitoring of filament wound pressure tanks during water-pressurizing test using embedded FBG sensor arrays. From the experimental results, it was demonstrated that FBG sensors can be successfully adapted to filament wound pressure tanks for their structural health monitoring by embedding.
© 2005 Elsevier Ltd. All rights reserved.

Keywords: FBG sensor; Filament wound; Pressure tank; Multiplexing; Embed

1. Introduction

Composite materials are increasingly being used as engineering materials in aircrafts, buildings, containers, and structures. In particular, the use of filament wound composite tanks is increasingly prevalent because of high specific strength and specific stiffness over their metal counterparts, as well as excellent corrosion and fatigue resistance. Filament wound composite tanks are finding their use in the applications such as fuel tanks, pressure tanks, and motor cases of aerospace structures.

The complexity in damage mechanisms and failure modes makes the use of composite materials difficult. Most of the conventional damage assessment and non-destructive inspection methods are time-consuming and are often difficult to implement on hard-to-reach-parts of the structure. For these reasons, a built-in assessment system must be developed to constantly monitor the structural integrity of critical components.

Electric strain gages (ESGs) have been generally used to monitor the strain behavior of pressure tanks. However, the increase of sensors caused complexity in handling and resulted in a measurement error due to a noise induced by long electric cables because many sensors were necessary for precise analysis of strain behavior.

Fiber optic sensors (FOSs) have shown a potential to serve real time health monitoring of the structures in many applications [1,2]. They can be easily embedded or attached to the structures and are not affected by electro-magnetic fields. In addition, they have not only the flexibility in the selection of the sensor size but also high sensitiveness. Recently, fiber optic sensors, especially FBG sensors, have been introduced into composite structures because FBG sensors based on wavelength division multiplexing (WDM) technology are attracting considerable research interest and appear to be ideally suitable for structural health monitoring of smart composite structures. FBG sensors are easily multiplexed and have many advantages such as linear response, absolute measurement, etc.

* Corresponding author. Tel.: +82 31 460 5760; fax: +82 31 460 5759.
E-mail address: dhkang@krri.re.kr (D.H. Kang).

0963-8695/$ - see front matter © 2005 Elsevier Ltd. All rights reserved.
doi:10.1016/j.ndteint.2005.07.013

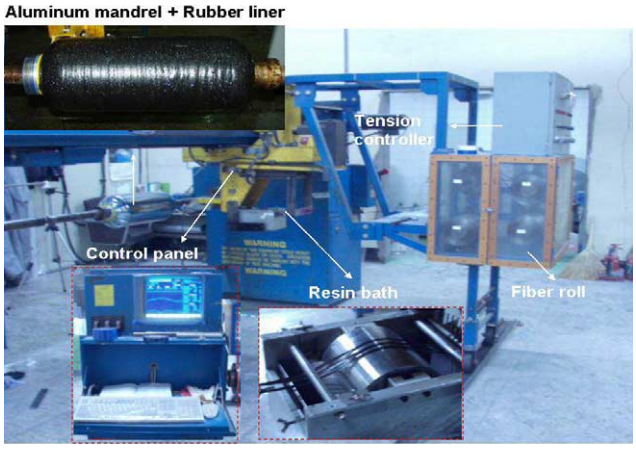

Fig. 1. Fabrication process of a filament wound pressure tank.

Foedinger et al. measured the temperature and strains during the cure and studied ingress/egress methods for a standard testing and evaluation bottle (STEB) using FBG sensors. Through a water-pressurizing test, experimental data were compared with the results of ESGs and finite element analysis (FEA) [3]. Lo et al. measured the unbalanced strain from the wavelength difference of a pair of FBG sensors during a water-pressurizing test. However, it was impossible to measure absolute strains at each sensor position [4]. Degrieck et al. embedded an FBG sensor between the hoop layers and measured the internal pressure of the tank through a water-pressurizing test from the wavelength shift of an FBG sensor. The lack of sensors limited strain measurements onto local positions. In addition, they conducted a 3-point bending test of carbon/epoxy composite laminate [5]. Kang et al. attached 32 FBG sensors on the filament wound pressure tank as four channels and measured the strains through a water-pressurizing test [6].

From the above literatures, we can find out that only a few FBG sensors were used when embedding sensors into the pressure tank and relatively a large number of FBG sensors were used when attaching sensors on the surface. Therefore, it is necessary to monitor the strains of a filament wound pressure tank using a number of embedded FBG sensors in real time.

In this paper, FBG sensor arrays were embedded into filament wound pressure tanks during the fabrication process and the techniques for higher survivability and signal stability were suggested. Through water pressurizing tests, measured strains from FBG sensors were compared with those from ESGs and FEM analyses.

2. Filament wound pressure tanks with embedded FBG sensor arrays

2.1. A preliminary fabrication—STEB1

During a wet winding process, it is very difficult to embed an FBG sensor line with accuracy because the viscosity of epoxy resin is low enough to flow. In addition, because of the applied tension in reinforcing fibers, embedded FBG sensors are easy to fail during the fabrication process. For the reason, a preliminary fabrication of a pressure tank was conducted in order to develop the embedding methods of FBG sensor lines with high survivability.

Fig. 1 shows a general fabrication process of a filament wound pressure tank. The equipments for the filament winding are composed of a tension controller which regulates the fiber tension, a resin bath, a fiber roll, and a control panel which commands the winding pattern, winding speed, etc. Before the main winding of the tank, rubber winding was conducted on an aluminum mandrel. The rubber liner made by rubber winding is necessary for the prevention of a leakage during the use of fabricated pressure tank. The winding tension was 1.5 kg/end and the bandwidth of hoop and helical layer was 10.0, 10.5(mm) for five-ends, respectively. The cylinder part includes a three-body helical layers and 5-body hoop layers so that

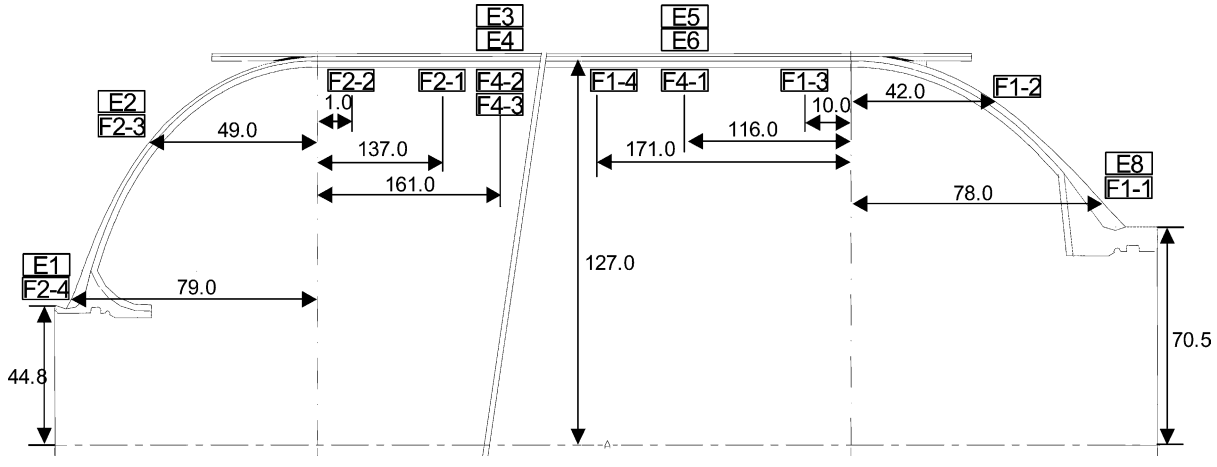

Fig. 2. Configurations and sensor positions about a preliminary fabrication.

Table 1
Comparison between the processes of previous and revised

Content	Process	
	Previous	Revised
Optical fiber	SMF+hydrogen loading	Photo-sensitive fiber
Multiplexing	Splicing	Simultaneous fabrication
Reinforcement	Recoat	Recoat+adhesive film
Ingress/egress	One direction	Both directions

the sequence is $[(\pm 27.5)_3/90_5]_T$ denoting from inner to outer layers.

Four FBG sensor lines were fabricated and each line was fabricated through an arc-fusion splicing with each FBG sensor. Each FBG sensor was fabricated using a single mode fiber (SMF) with high photosensitivity through a high temperature hydrogen loading process and then it was recoated with acrylate. The channel 1(CH1) and channel 2(CH2), each has 4 FBG sensors, were embedded between the layer 1 and 2 at aft dome and the layer 2 and 3 at forward dome, respectively. The channel 3(CH3) and channel 4(CH4), each has three FBG sensors, were embedded into a cylinder part, respectively. Since most of the loading applied to a pressure tank is sustained by reinforcing fibers, it is important to measure the strains along the fiber direction. Hence, all FBG sensors were aligned to fiber directions of the pressure tank except three sensors of CH3 embedded in perpendicular to the reinforcing fiber direction at the cylindrical part. The experimental model is the standard testing and evaluation bottle (STEB) and the configurations including sensor positions are shown in Fig. 2. From Fig. 2, 'F' denotes FBG sensor and 'E' denotes ESG. And, the figure following 'F' means the channel number.

After the curing process is completed, the survivability of FBG sensors and their reflected signals were examined through an optical spectrum analyzer (OSA) for each channel. From the results, no signal was detected at the channel 1, and channel 3 was broken during the embedding process while FBG sensor signals were detected at the channel 2 and 4 after curing process. However, CH2 was also failed at the ingress/egress point during handling the tank. Among the survived sensors, the intensity reduction was observed during the embedment. From the experimental results of a preliminary fabrication, it is confirmed that FBG sensors are to be easily failed from many causes in their embedment. Therefore, the improvement of sensor survivability is the most important for the embedment of FBG sensors into a filament wound pressure tank.

2.2. Improvement of sensor survivability—STEB2

In this paragraph, a new fabrication process of FBG sensors that is focused on the improvement of sensor survivability is introduced. Several processes concerning the embedment of sensor lines were revised, as shown in Table 1.

Fig. 3. An FBG sensor line protected with arcylate recoating and adhesive film.

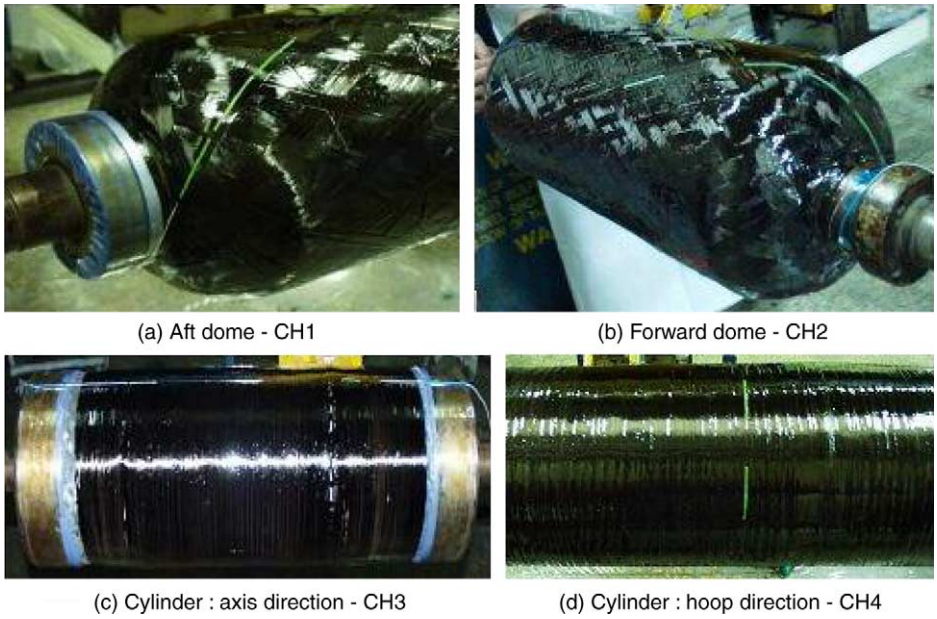

Fig. 4. Embedded FBG sensor lines during the fabrication.

First, an optical fiber used for fabricating an FBG sensor was substituted to a photosensitive optical fiber (PS1250/1500, Fibercore) because the hydrogen loading process of optical fibers affected on the mechanical strength of them [7]. Second, a sensor line with multiple sensors was fabricated not by the splicing between FBG sensors, but by a simultaneous fabrication of FBG sensors in a single fiber. Generally, optical fibers connected by acr-fusion splicing are very weak to the transverse stress at the splicing point. Third, as a reinforcement of FBG sensors during the embedment, the protection with an adhesive film was conducted as a second protection process after recoating. Lastly, optical fibers were extracted from a filament wound pressure tank towards both directions of a sensor line. It was because optical fiber lines were the weakest at the ingress/egress point after the end of curing process.

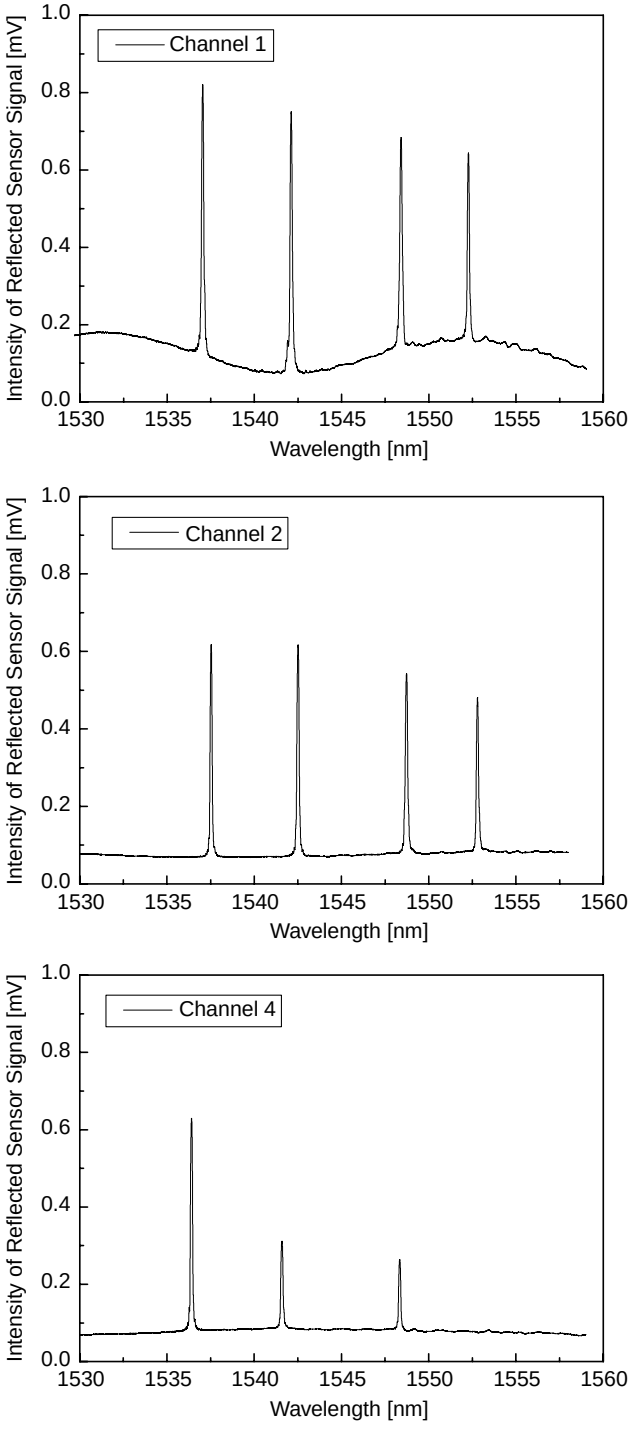

Fig. 5. Reflected spectra of FBG sensors of Ch1, 2, 4.

As mentioned in the above paragraph, multiple FBG sensors were fabricated in a single optical fiber in order to increase the accuracy of sensor position and to decrease the strength degradation of optical fiber caused by arc-fusion splicing between optical fiber segments. Fig. 3 shows an FBG sensor line fabricated by a revised fabrication process listed in Table 1. Fig. 4 shows the embedded sensor lines during the fabrication process. After embedding each sensor line, embedding positions of FBG sensors were measured accurately using a laser pointer. The filament wound pressure tank with embedded FBG sensor lines were cured under rotating condition in the curing cycle; 80 °C (1 h)→120 °C (1 h)→150 °C (3 h) in an oven.

When the tank was completely fabricated, 11 of 14 sensors survived. Three sensors of CH3 failed during the cure as shown in Fig. 5. Though some sensors showed a little intensity loss of reflected signal during the cure, they did not fail. From the wavelength shift of an FBG sensor between before and after curing, residual strains were measured at all sensor positions. As shown in Table 2, compressive strains were measured at all positions and the strain values were about hundreds of micro strains and the residual strain values in forward dome were relatively higher.

After fabricating a pressure tank, a water-pressurizing test of STEB2 was performed with the tank to its burst. Fig. 6 depicts the experimental setup for the strain monitoring of a tank during hydrostatic pressurization. The strain measurement was performed at intervals of 100 psi up to the burst. On the domes, four ESGs were attached on the surface at the same locations of embedded FBG sensors, aligned to the helical winding direction. On the cylinder, also four ESGs were attached in the hoop

Table 2
Residual strains of STEB2

Channel	Sensor No.	Residual strain (με)
CH1	F1-1	−359
	F1-2	−158.4
	F1-3	−11.5
	F1-4	−136.8
CH2	F2-1	−492.5
	F2-2	−522.9
	F2-3	−580.6
	F2-4	−485.0
CH4	F4-1	−401.2
	F4-2	−302.1
	F4-3	−503.9

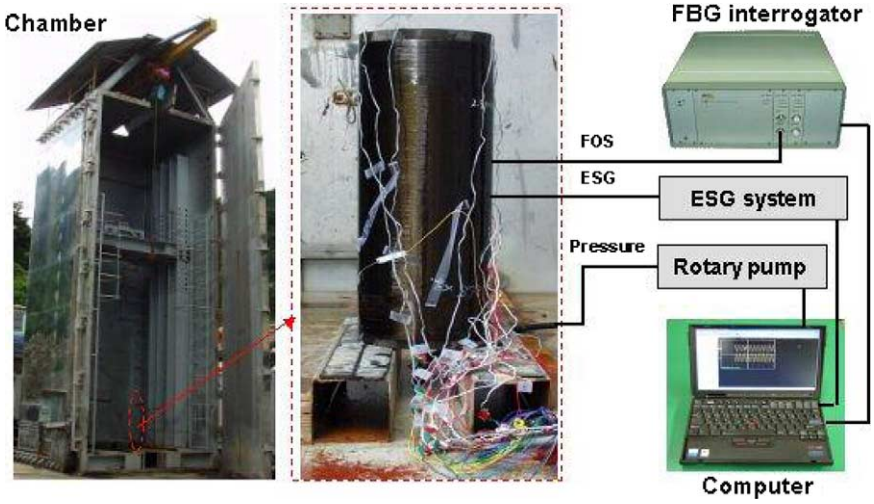

Fig. 6. Experimental setup for a water pressurizing test.

winding direction, i.e., the circumferential direction of cylinder. The signals of the FBG sensors, strain gauges, and a pressure transducer were acquired simultaneously by computers, processed and displayed by a signal-processing program written in LabVIEW® software. The specifications of used FBG sensor system are shown in Table 3.

FBG sensors were failed earlier than the burst of a pressure tank during the burst test. The maximum strains measured by FBG sensors during the burst test showed a large deviation. Above all, because strain gradients induced by the geometry of a forward dome generated peak splits of embedded FBG sensors, strains were measurable only at a low pressure. Considering the peak split, the maximum strains measured by FBG sensors during the burst test are listed in Table 4. Because of this, the signal stability of FBG sensors during the embedment is very important. The burst of STEB2 occurred at the pressure of 3430 psi. As shown in Fig. 7, the failure occurred near the boss of an aft dome and the aluminum boss was separated.

Table 3
Specifications of an FBG interrogations system

IS-7000 FBG Interrogator (FiberPro Co.)	
Wavelength range	35 nm (1530–1565 nm)
Avg. output power	3 mW
Resolution	<2 pm
Measurement speed	200 Hz
# of channels	8
Temperature range	10–40 °C

Table 4
Maximum measured strains during the burst test

Channel	Sensor no.	Max. measured strain (pressure)
CH 1	F1-1	0.95% (2900 psi)
	F1-2	0.90% (2900 psi)
	F1-3	0.80% (2900 psi)
	F1-4	0.90% (2900 psi)
CH 2	F2-1	0.67% (1400 psi)
	F2-2	0.52% (1400 psi)
	F2-3	0.32% (900 psi)
	F2-4	0.35% (1000 psi)
CH 4	F4-1	0.58% (1400 psi)
	F4-2	0.62% (1400 psi)
	F4-3	0.60% (1400 psi)

3. Finite element modeling

Finite element analyses on STEB were done by a commercial code, ABAQUS. In this research, the 3-D layered solid element was utilized and the boundary condition was considered as cyclic symmetric. Fig. 8 shows the detailed FEA model of STEB realized by a commercial code, PATRAN, and the material properties of T700/Epoxy used in the analysis are as follows. $E_1=$ 134.6 GPa, $E_2=7.65$ GPa, $G_{12}=3.68$ GPa, $\nu_{12}=0.3\sigma_f=$ 2290 MPa, $\sigma_t=31.8$ MPa, $S=75.8$ MPa

The modified Hashin's failure criterion was selected and applied to progressive failure analysis. For the purpose of failure analysis, a subroutine, USDFLD of ABAQUS ver 6.3 was coded to define the change of mechanical properties due to failure.

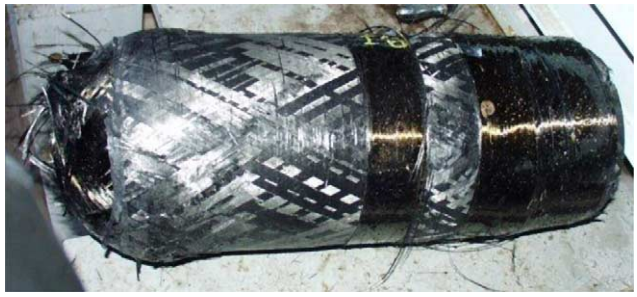

Fig. 7. The failure shape of STEB2.

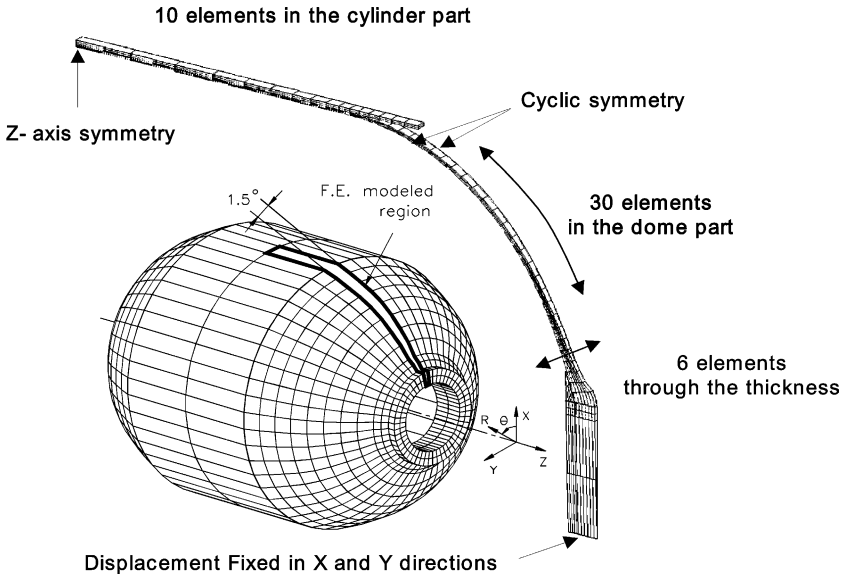

Fig. 8. The FEA model of STEB.

4. Experimental results

Fig. 9 shows a strain result measured by FBGs and ESGs in cylinder part up to 500 psi. The results from FBG sensors were compared with those from ESGs which were attached at the same longitudinal locations with FBG sensors. The strain measured by each FBG sensor showed a good linearity with the increase of pressure and showed little difference with that by an ESG. Fig. 10 shows the strain results measured by FBGs, ESGs, and FEA at 500 psi. Both strain results were also compared with those of FEM analyses, which were indicated as lines in Fig. 10.

Considering only the FEA results, helical layers of front dome and aft dome showed a large difference in strains between inner and outer layers. However, there was little difference in strains between inner and outer layers at cylinder part.

In Fig. 10, the strains measured by FBGs and ESGs were similar at hoop layers of cylinder part and also showed a good agreement with the FEA results, while the results from FBGs and ESGs at both domes showed a large difference with each other. At dome parts, only a little change of longitudinal position can cause large changes in strain values. The differences in strains measured by FBG sensors and ESGs may be occurred by a mismatch of attaching angles and locations between them. In addition, these differences may be caused by the slippage of an embedded FBG sensor line during the curing process due to resin flow. Fig. 11 shows the FEA analysis against the experimental data as the embedding angle of an FBG sensor line (CH1) changes. From the result of Fig. 11, the CH1 seemed to be slipped about 10 from the reinforcing fiber direction during the embedment.

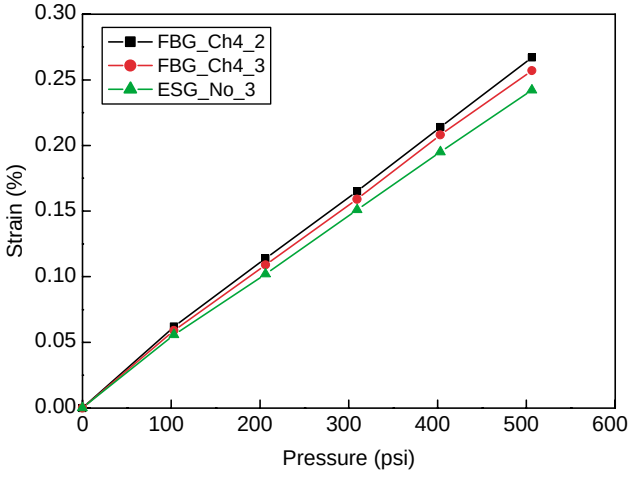

Fig. 9. The strain result of FBGs and ESGs at cylinder part.

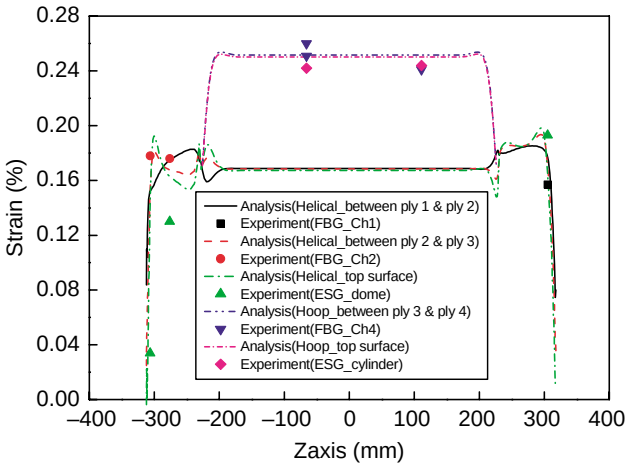

Fig. 10. The strain results of FBGs, ESGs, and FEA at 500 psi.

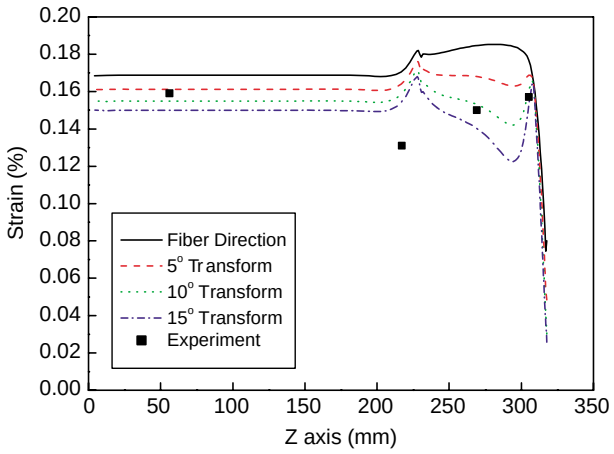

Fig. 11. Analysis on the cause of strain measurement errors—aft dome.

When embedding FBG sensors into a filament wound pressure tank, especially a dome part, the signal stability of FBG sensors is very important for the strain measurement at a high-pressure level, as was confirmed in the fabrication results of STEB2. FBG sensors with shorter grating lengths are more stable and effective when they are under strain gradients [8] and are embedded perpendicular to the reinforcing fibers. For the reason, FBG sensors with shorter grating lengths should be embedded in dome parts of filament wound pressure tanks in order to measure the strains during the operation without peak splits induced by strain gradients.

5. Statistics of sensor failure

As mentioned in the above paragraph, FBG sensors with shorter grating length are more effective in the existence of strain gradient. Moreover, the survivability of FBG sensors becomes higher when they are embedded perpendicular to the reinforcing fiber of composites. In this study, we fabricated another STEB using FBG sensors with the grating length of 5 mm, which were fabricated using a reflection prism. Fig. 12 shows the experimental setup for the fabrication of FBGs with shorter grating length. The reflectivity of the special coating on the surface of a prism is more than 99% at the wavelength of 248 nm. Therefore, only a part of incident light not reflected at the prism can get to the phase mask and the grating length can be adjusted by moving the three-axis translation stage on which the reflection prism is located.

A STEB3 which was fabricated using FBG sensors with the grating length of 5 mm showed 100% survivability of FBG sensors during the whole fabrication step and no peak split also occurred through a water-pressurization test. Nevertheless, FBG sensors are very easy to fail from the fabrication to the operation due to several causes. In order to analyze the main causes of FBG sensor failure, five tanks were additionally fabricated except the above tanks (STEB1 and 2). The configurations and the number of embedded FBG sensors of each tank are different a little with its objectives of the application. The fabrication results are shown in Table 5.

Through the fabrication of five tanks, 61 of 75 sensors survived. Therefore, the net survivability was about 81%. As shown in Fig. 13, the main causes of FBG sensor failure could be listed as ‘winding processes’, ‘curing process’, and ‘handling process’. Most of the failure occurred during handling, especially at the ingress/egress point. From the result, the protections of grating parts and ingress/egress point seem to be the most important for the successful application of FBG sensors to filament wound pressure tanks by embedding.

6. Conclusions

In this paper, filament wound pressure tanks with embedded FBG sensor arrays were fabricated. The present study can be summarized and conclude as follows:

1 It is necessary to fabricate an FBG sensor line with a revised fabrication process for higher sensor

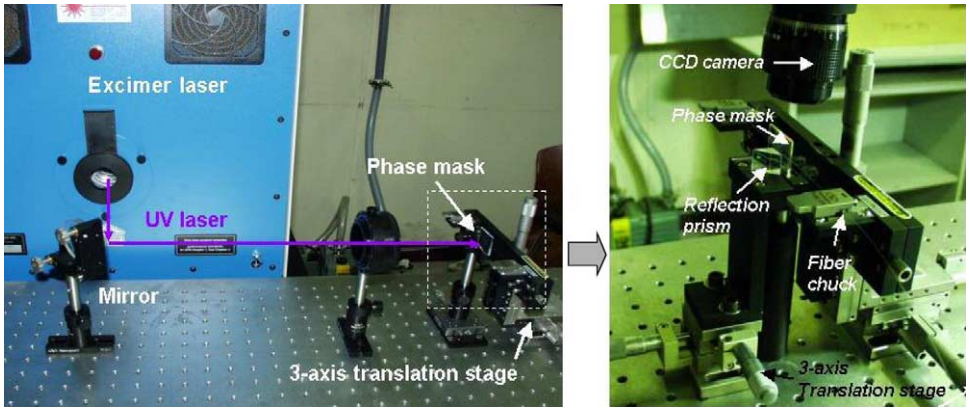

Fig. 12. Experimental setup for the fabrication of FBGs with shorter grating length.

Table 5
Survivability of embedded FBG sensors

Model	Content		
	Attempt	Survival	Survivability (%)
STEB3	22	22	100
STEB4	12	6	50
STEB5	12	8	67
STEB6	15	15	100
STEB7	14	10	71
Total	75	61	81

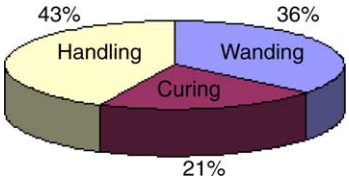

Fig. 13. The causes of FBG sensors failure.

survivability when it is embedded into a filament wound pressure tank.

2 Residual strains of a filament wound pressure tank are about hundreds of micro strains in compressive at all positions and are relatively higher in forward dome.

3 FBG sensors embedded into dome parts can fail earlier than the burst of a pressure tank because of the strain gradient induced by their geometry and it can be prevented using FBG sensors with shorter grating length.

4 The strains measured by FBGs and ESGs were similar at hoop layers of cylinder part and also showed a good agreement with the FEA results though the slippage of an FBG sensor line in dome parts during the cure caused some measurement errors during the water-pressurizing test.

From the results, it was demonstrated that FBG sensors could be successfully adapted to filament wound pressure tanks for their structural health monitoring by embedding.

Acknowledgements

This paper was performed for the Hydrogen Energy R&D Center, one of the 21st Century Frontier R&D Program, funded by the Ministry of Science and Technology of Korea.

References

[1] Okabe Y, Tsuji R, Takeda N. Application of chirped fiber Bragg grating sensors for identification of crack locations in composites. Compos Part A Appl Sci Manuf 2004;35(1):59–65.

[2] Liu T, Fernando GF. Processing of polymer composites: an optical fibre-based sensor system for on-line amine monitoring. Compos Part A Appl Sci Manuf 2001;32(11):1561–72.

[3] Foedinger RC, Rea DL, Sirkis JS, Baldwin CS, Troll JR, Grande R, et al. Embedded fiber optic sensor arrays for structural health monitoring of filament wound composite pressure vessels. Proc SPIE 1999;3670:289–301.

[4] Lo YL, Sung PH, Wang HJ, Chen LW. Pressure vessel wall thinning detection using multiple pairs of fiber Bragg gratings for unbalanced strain measurements. J Nondestr Eval 2000;19(3):105–13.

[5] Degrieck J, De Waele W, Verleysen P. Monitoring of fibre reinforced composites with embedded optical fibre Bragg sensors, with application to filament wound pressure vessels. NDT&E Int 2001;34: 289–96.

[6] Kang HK, Park JS, Kang DH, Kim CU, Hong CS, Kim CG. Strain monitoring of filament wound composite tank using fiber Bragg grating sensors. Smart Mater Struct 2002;11(6):848–53.

[7] Wei CY, Ye CC, James SW, Tatam RP, Irving PE. The influence of hydrogen loading and the fabrication process on the mechanical strength of optical fibre Bragg gratings. Opt Mater 2002;20:241–51.

[8] Kang DH, Park SO, Hong CS, Kim CG. The signal characteristics of reflected spectra of fiber Bragg grating sensors with strain gradients and grating lengths. NDT&E Int 2005; accepted for publication.